AEROSPACE REPORT NO
TOR-0066(5758-02)-3

AD708147

A Comparison of Four Simple Calculation Methods for the Compressible Turbulent Boundary Layer on a Flat Plate

Prepared by B. PEARCE
Applied Mechanics Division,
Engineering Science Operations

70 MAR 16

Prepared for SPACE AND MISSILE SYSTEMS ORGANIZATION
AIR FORCE SYSTEMS COMMAND
LOS ANGELES AIR FORCE STATION
Los Angeles, California

Contract No. F04701-69-C-0066

Systems Engineering Operations
THE AEROSPACE CORPORATION

THIS DOCUMENT HAS BEEN APPROVED FOR PUBLIC RELEASE AND SALE: ITS DISTRIBUTION IS UNLIMITED

DDC
RECEIVED
JUL 8 1970
C

Report No.
TOR-0066(5758-02)-3

A COMPARISON OF FOUR SIMPLE CALCULATION METHODS FOR THE COMPRESSIBLE TURBULENT BOUNDARY LAYER ON A FLAT PLATE

Prepared by

Blaine Pearce
Applied Mechanics Division
Engineering Science Operations

70 MAR 16

Systems Engineering Operations
THE AEROSPACE CORPORATION
El Segundo, California

Prepared for

SPACE AND MISSILE SYSTEMS ORGANIZATION
AIR FORCE SYSTEMS COMMAND
LOS ANGELES AIR FORCE STATION
Los Angeles, California

Contract No. F04701-69-C-0066

This document has been approved for public release and sale; its distribution is unlimited

Report No.
TOR-0066(5758-02)-3

A COMPARISON OF FOUR SIMPLE CALCULATION METHODS FOR THE COMPRESSIBLE TURBULENT BOUNDARY LAYER ON A FLAT PLATE

Approved

W. F. Radcliffe, Director
Engineering Analysis Subdivision
Applied Mechanics Division

J. H. Ashmore, Director
Development Office
Advanced Vehicle Systems Directorate
Systems Planning Division

The information in a Technical Operating Report is developed for a particular program and is therefore not necessarily of broader technical application.

ABSTRACT

Four simple calculation procedures for estimating the heat transfer and skin friction for a turbulent compressible boundary layer on a smooth flat plate are compared with experimental data in flows approximating the boundary layer edge conditions on the bottom surface of the Space Transportation System orbital vehicle. The methods compared are Eckert's reference enthalpy, the adiabatic wall reference enthalpy, Spalding and Chi, and the reference density-viscosity ($\rho\mu$)-method. For the data used in this comparison the most consistently accurate prediction of the skin friction is given by Spalding and Chi's method. This method also gives the best estimates of the heat transfer when used with Von Karman's equation for the Reynolds analogy factor. In general, the estimates from Spalding and Chi's method with the Von Karman form of the analogy factor are within ± 20 percent of the measured values of the heat transfer. The choice of an effective origin for the turbulent boundary layer is examined and an origin defined by matching the laminar and turbulent momentum thicknesses at a point halfway between onset and completion of transition or an origin at the onset of transition improves the heating estimates in the initial region of fully turbulent flow. It is emphasized that the predictions examined in this report, since they are applicable only to a flat plate with uniform boundary layer edge conditions, account only for the effects of variable density and transport properties in a turbulent boundary layer.

CONTENTS

I.	INTRODUCTION	1
II.	OBJECTIVE AND EXTENT OF THE COMPARISON	2
III.	BOUNDARY LAYER EDGE CONDITIONS	5
IV.	REVIEW OF THE CALCULATION METHODS	6
V.	EXPERIMENTAL DATA	12
VI.	COMPARISON WITH SKIN FRICTION DATA	14
VII.	REYNOLDS ANALOGY	21
VIII.	COMPARISON WITH HEAT TRANSFER DATA	24
IX.	EFFECTIVE ORIGIN OF TURBULENT FLOW	34
X.	SUMMARY AND CONCLUSIONS	38
NOMENCLATURE		41
REFERENCES		43

TABLES

1. Boundary Layer Edge Conditions at Peak Turbulent Heating 5

2. Summary of the Features of the Four Calculation Methods . . . 9

3. Skin Friction Predictions According to the Three Skin Friction Laws ($c_f^* \times 10^3$) 10

4. Summary of Experimental Data 13

5. Range of Relative Errors in the Comparison with Skin Friction Data from Ref. 3 (error in %) 16

6. Comparison with Skin Friction Data Made by Spalding and Chi in Ref. 11 (error, percent, root-mean-square) 16

7. Range of Relative Errors in the Comparison with Skin Friction Data from R f. 5 (error in %) 17

8. Average Reynolds Analogy Factors from Ref. 5 21

9. Range of Relative Errors in the Comparison with Heat Transfer Data from Ref. 5 (error in %) 26

10. Displacement Thicknesses on the Inside of the Tube Wall 28

11. Percent of the Predictions Which Give Relative Errors Within ±15 Percent of the Heat Transfer Data from Ref. 7 . . . 32

FIGURES

1.	Comparison of Measured and Calculated Skin Friction.	15
2.	Comparison of Measured and Calculated Skin Friction on an Adiabatic Wall	18
3.	Comparison of Measured and Calculated Skin Friction.	19
4.	Reynolds Analogy Factor	22
5.	Comparison of Measured and Calculated Heat Transfer	25
6.	Comparison of Measured and Calculated Heat Transfer	29
7.	Comparison of Measured and Calculated Heat Transfer	31
8.	Comparisons of Different Effective Origins for the Turbulent Boundary Layer	36
9.	Comparison of Different Effective Origins for the Turbulent Boundary Layer	37

I. INTRODUCTION

Analyses of preliminary designs of the Space Transportation System (STS) orbital vehicle have shown that aerodynamic heating is an essential factor in determining the feasibility of a large lifting orbital vehicle which is protected during reentry by a metal reradiative heat shield that must be reused without extensive refurbishment. It is known that the highest temperatures during entry occur at stagnation points and leading edge regions, where the boundary layer is laminar. However, these regions are a small fraction (5 percent) of the total vehicle surface area and can be protected by materials that require more extensive refurbishment than what is feasible for the remainder of the vehicle. That portion of the vehicle which essentially determines the feasibility of a reusable heat shield is the bottom surface. This region is about 40 percent of the total vehicle surface and is by far the largest area exposed to heating rates which give surface temperatures near the limiting temperatures of those materials suitable for multiple use. Analyses have shown that peak heating over much of this surface occurs when the boundary layer is turbulent.

The reusability of a reradiative metal panel is determined essentially by the peak temperatures to which it is exposed. In addition, the vehicle plan form loading, optimum angle of attack and bank angle and the resulting potential cross-range are adversely affected by a decrease in the allowable peak temperature on the bottom surface. It is therefore necessary to obtain an accurate estimate of turbulent heating rates in order to be able to use for design purposes the full potential temperature range of the reradiative shield without having to allow an unusually large margin for uncertainty in the predicted temperatures. For this reason the prediction of turbulent heating rates assumes an important role in the design of an STS orbital vehicle.

II. OBJECTIVE AND EXTENT OF THE COMPARISON

The calculations which have been done for the turbulent boundary layer on the STS orbital vehicle have all utilized those estimates that are strictly valid for two-dimensional flow over a smooth flat plate. The use of these estimates is suggested by the fact that the bottom surfaces of the proposed orbital vehicles have very little longitudinal or transverse curvature. There is essentially no longitudinal pressure gradient except near the nose and the region of interest for turbulent flow is sufficiently far downstream from the nose region that the initial development of the boundary layer is not expected to have a large effect on the turbulent boundary layer far downstream. More importantly, the orbiter configurations are nearly delta-wings (at least in the forward portion of the vehicles) and there is a transverse component of flow in the boundary layer due to the three-dimensional flow at the boundary layer edge. But, for a turbulent boundary layer, the increase in heating due to the cross-flow can be accounted for by a small correction (less than 20 percent for angles of attack less than 60 deg) to the heating without cross-flow. In particular, this approximation is valid along the centerline and for very cold walls. Moreover, at this time the STS is in a preliminary design phase that requires a large number of heating calculations, usually done in conjunction with trajectory calculations, and elaborate computation schemes are not yet warranted. For these reasons the turbulent boundary layer on the bottom of the STS orbiter has been approximated by that on a flat plate with no pressure gradient, even though the accuracy of this approximation is not really known. Since all the effects which cause the turbulent boundary layer on the orbiter bottom surface to be different from that on a flat plate in a uniform stream are either ignored or accounted for by a small correction, the major factor which must be accounted for in the heating estimates is the fact that the fluid in the boundary layer has variable density and variable transport properties.

It is the objective of this report to select from a group of simple methods for turbulent boundary layer heat transfer estimates the one which most correctly accounts for the compressibility and variable fluid properties for a flat plate in a uniform flow with boundary layer edge conditions and wall conditions typical of those expected for the STS orbiter bottom surface. This will be accomplished by comparing the predictions from each method with experimental data that approximately coincide with the applicable flow conditions. There are four calculation methods to be compared:

1. Eckert reference enthalpy
2. Adiabatic wall reference enthalpy
3. Reference density-viscosity product ($\rho\mu$)
4. Spalding-Chi

These particular methods are used because they are the ones used by the contractors participating in the STS study. In addition, they are representative of the other methods of this type.

In addition to the comparison of the four heating methods, a brief estimate of the effect of the origin of the turbulent boundary layer is given. The effect of using different origins is examined and the predictions are compared with experimental data for the initial region of fully turbulent flow. The error which occurs when the leading edge of the vehicle is used as an origin rather than a more realistic value at or downstream from the point of transition onset is comparable to the difference in heating predictions from the various methods. It is therefore appropriate to consider the effect of the origin for the turbulent boundary layer along with the calculation method.

Other comparisons similar to the one given here have already been made (Refs. 1, 2, 3). The present comparison was made in order to examine the accuracy of these four specific methods. Also, the preliminary analyses have allowed a fairly precise definition of the boundary layer edge conditions and wall temperature range for the STS orbiter which allows the comparison to be made in a rather restricted range of boundary edge Mach number,

Reynolds number, and wall temperature. The present comparison is therefore able to emphasize a small range of boundary layer and wall conditions in contrast to previous studies, which have been of a more general nature. Because of the emphasis on a more restricted range of wall conditions and because the present comparison includes the adiabatic wall reference enthalpy method in addition to the three more commonly used methods, the present comparison is complementary to the previous work.

III. BOUNDARY LAYER EDGE CONDITIONS

The previous investigations of these computational methods have shown that the accuracy of the predictions can vary widely with Mach number and the degree of wall cooling. This suggests that in the present comparison one can expect accurate estimates by a particular method for only a restricted set of boundary layer conditions. The particular boundary layer edge conditions which are expected to occur near peak heating for the STS orbiter can be defined in order to isolate the conditions of primary interest.

Vehicle angles of attack of from 15 to 60 deg have been proposed, with the most important range being between about 30 to 60 deg. This implies boundary layer edge Mach numbers between about 7 and nearly unity, with the important range being between 5 and about 2. Reynolds numbers based on distance to the leading edge should be near the values for onset of fully turbulent flow which is about 2×10^6. The full range of Reynolds number is probably from about 10^6 to nearly 10^7. An additional parameter which is very important is the ratio of wall to adiabatic wall enthalpy. For wall temperatures of 2200°F and less and flight velocities at peak turbulent heating near 17,000 ft/sec, this ratio can be between about 0.12 and 0.06. These conditions are summarized in the following table.

Table 1. Boundary Layer Edge Conditions at Peak Turbulent Heating

Mach number	$1 \leq M_1 \leq 7$
Reynolds number	$10^6 < \frac{\rho_1 u_1 x}{\mu_1} < 10^7$
Wall enthalpy ratio	$0.06 \leq h_w/h_{aw} \leq 0.12$

IV. REVIEW OF THE CALCULATION METHODS

The four calculation methods to be compared are not really distinct from one another in the sense that all make use of the same basic hypothesis. It is supposed that there is a correspondence between a turbulent boundary layer in a compressible fluid with variable transport properties and a flow with uniform density and transport properties. In each case the correspondence is established by evaluating the density and transport properties of the uniform property flow at a reference enthalpy defined by the conditions of the real, compressible flow. The well-established relations for skin friction and heat transfer in a constant property turbulent boundary layer are then applied. In a strict sense, the four calculation procedures all use the same method; the essential differences are the choice of reference enthalpy and the relations which establish the transformation between the skin friction and Reynolds number in the compressible and incompressible boundary layers.

For an incompressible fluid with uniform properties the skin friction coefficient for a fully turbulent boundary layer on a flat plate is given by a relationship of the form

$$c_f^* = f(Re_x^*)$$

where the superscript * will be used to indicate a boundary layer with uniform density and transport properties. The calculation methods suppose that the friction coefficient for a compressible turbulent boundary layer is given by the same relationship when the friction coefficient and Reynolds number in the compressible flow are transformed to an equivalent flow with uniform density and transport properties evaluated at a reference enthalpy. The transformation is of the form

$$c_f^* = F_c\, c_f$$

$$Re_x^* = F_{Rx}\, Re_x .$$

The momentum thickness Reynolds number also transforms according to

$$Re_{\theta}^{*} = F_{R\theta}\, Re_{\theta}$$

where

$$F_{R\theta} = F_{c}\, F_{Rx}.$$

Heat transfer rates are then calculated by means of Reynolds analogy to obtain

$$St^{*} = k\,\frac{c_{f}^{*}}{2}$$

where k is the Reynolds analogy factor and the Stanton number, St*, in the incompressible flow is related to that in the compressible flow according to

$$St^{*} = F_{c}\, St.$$

There are two widely accepted expressions for the Reynolds analogy factor for an incompressible flow over a flat plate with uniform temperature:

1. Colburn's equation, $k = \sigma^{*-2/3}$
2. Von Karman's equation, $k = \left\{ 1 + 5\sqrt{\frac{c}{2}f^{*}}\left[(\sigma^{*} - 1) + \ln\frac{(5\sigma^{*} + 1)}{6}\right]\right\}^{-1}$

Since Reynolds analogy is used, the predictions are strictly applicable to boundary layers with no pressure gradient and a uniform wall temperature. They are, however, commonly used to estimate heating in the presence of slight pressure gradients and non-uniform wall temperatures. The $\rho\mu$-method, with additional transformations of the Reynolds number, has been proposed as a method applicable for variable pressure and wall temperatures (Ref. 8).

Expressions for the quantities F_c, F_{Rx}, $F_{R\theta}$ and the reference enthalpy are given in Table 2. The adiabatic wall reference enthalpy is obtained from Eckert's by replacing the wall enthalpy by the adiabatic wall enthalpy. In Spalding and Chi's prediction, the skin friction multiplier, F_c, requires an integration of the density distribution through the boundary layer. For this calculation, the total enthalpy profile was taken to be a linear function of the velocity. The $\rho\mu$-reference enthalpy requires some empirical relations between the density-viscosity products at the wall, boundary layer edge, and stagnation conditions to evaluate the reference enthalpy. Details of this calculation are given in Ref. 8. For all of the subsequent calculations, the predictions for each of these methods were evaluated using real gas properties with the exception of the Prandtl number, which was taken to be a constant value of 0.715.

A choice of the low-speed skin friction law is essentially independent of the particular method. However, each method has usually been associated with a particular law, and these are indicated in Table 2 and are summarized below.

1. Spalding-Chi (Tabular)
2. Prandtl, $c_f^* = 0.0592\ Re_x^{*-1/5}$
3. Modified Schultz-Grunow, $c_f^* = 0.37\ [\log_{10}(Re_x^* + 3000)]^{-2.584}$

A completely consistent comparison should use the same law for each method. However, this refinement is not made here. The differences between the skin friction predicted by each method in the Reynolds number range of interest are illustrated by the values for each law given in Table 3. The deviation of one law from another can be as large as 15 percent for this range of Reynolds numbers. Of the three laws, Spalding and Chi's and the modified Schultz-Grunow equation are probably the most accurate (Ref. 12).

Table 2. Summary of the Features of the Four Calculation Methods

Method (Reference)	F_c	F_R	$F_{R\theta}$	h^*	Skin Friction Law
Eckert (9)	ρ_1/ρ^*	$\frac{\rho^*\mu_1}{\rho_1\mu^*}$	μ_1/μ^*	$\frac{1}{2}(h_w+h_1)+0.22r(h_o-h_1)$	Prandtl
Adiabatic Wall (10)	ρ_1/ρ^*	$\frac{\rho^*\mu_1}{\rho_1\mu^*}$	μ_1/μ^*	$h_1 + 0.72r\,(h_o-h_1)$	Prandtl
Spalding-Chi (11)	$\left[\int_0^1 \left(\frac{\rho}{\rho_1}\right)^{1/2} d\left(\frac{u}{u_1}\right)\right]^{-2}$	$\frac{F_{R\theta}}{F_c}$	$\left(\frac{h_w}{h_1}\right)^{-0.702}\left(\frac{h_{aw}}{h_w}\right)^{0.772}$	----------	Tabular Values (11)
$\rho\mu$ (8)	$\frac{\rho_1\mu_o}{\rho^*\mu^*}$	$\frac{\rho^*\mu_1\mu^*}{\rho_1\mu_o^2}$	μ_1/μ_o	----------	Modified Schultz-Grunow

Table 3. Skin Friction Predictions According to the Three Skin Friction Laws ($c_f^* \times 10^3$)

Re_x^*	Spalding-Chi	Modified Schultz-Grunow	Prandtl
1.006×10^4	9.00	9.56	9.37
1.417×10^5	5.00	5.33	5.52
1.062×10^6	3.50	3.57	3.69
0.34×10^6	2.50	2.45	2.39
4.651×10^7	2.00	1.92	1.73

There are two ways in which these calculation procedures can be interpreted for the purpose of determining the heat transfer. The first is that Reynolds analogy should be strictly true and the most accurate method is the one giving the best prediction of both heat transfer and skin friction. Alternatively, Reynolds analogy can be regarded as only suggesting a correlation of heat transfer which must satisfy the true analogy only when the conditions for its validity are strictly satisfied. It is this latter view to which one is forced in order to obtain an adequate approximation for the heat transfer using these simple methods. For this reason both skin friction and heat transfer are considered in the subsequent comparison and it is possible to suggest an effective analogy factor that compensates for errors in the skin friction coefficient predictions to achieve a more accurate heat transfer prediction.

V. EXPERIMENTAL DATA

If an ideal set of experimental data existed, that is, data for either heat transfer or skin friction in fully turbulent flow over a flat plate, which was free from experimental errors and matched precisely the boundary layer edge conditions and wall enthalpy ratios of interest, then one of the four methods could be clearly distinguished as that which most accurately accounts for the effects of variable density and transport properties in a turbulent boundary layer. Unfortunately, no such set of data exists and the issue of determining the most accurate prediction cannot be unambiguously resolved. In each of the experiments there is the question of the effects of pressure gradient, origin of the boundary layer, and of course, experimental error. In addition, the most reliable data does not correspond precisely to the applicable boundary layer edge conditions or wall enthalpy ratio and that data which does correspond closely has some form of uncertainty which renders it less reliable for the present purpose. The conclusions reached in this report are therefore subject to these limitations imposed by the experimental data. Moreover, the conclusions could be altered if the comparison could be based on more accurate data at the precise conditions for the turbulent boundary layer on the STS orbiter.

The data used in the present comparison is not extensive and was chosen to illustrate specific points and to complement the comparisons made in previous work (Refs. 1, 2, and 3). In addition, the effect of the wall enthalpy ratio is emphasized more than that due to the Reynolds number or Mach number. The data is summarized in the following table along with the boundary layer edge conditions and wall enthalpy ratios.

Table 4. Summary of Experimental Data

Reference	Measured Quantity	M_1	Re_x, Re_θ	h_w/h_{aw}	Configuration
3	c_f	6.5, 7.4	Re_θ 2.26×10^3 - 6.25×10^4	0.31 - 0.51	Flat Plate
4	c_f	1.48-5.79	Re_θ 2.34×10^3 - 3.78×10^4	1	Flat Plate or Wind Tunnel Wall
5	c_f, St	4.26-10.7	Re_x 2.5×10^6 - 6×10^7	0.137 - 0.262	Flat Plate
6	St	2.5-3.5	Re_x 10^5-10^6	0.01 - 0.04	Inside of a Cylinder
7	St	1.79-2.31	Re_x 1.5×10^6 2×10^7	0.045 - 0.134	Inside of a Cylinder

VI. COMPARISON WITH SKIN FRICTION DATA

The skin friction predictions from each of the methods will be compared with experimental data because this is just as useful in determining the accuracy of the predictions as is the comparison for heat transfer. Furthermore, one element of uncertainty, the Reynolds analogy factor is removed and if the comparison is based on a momentum thickness Reynolds number, the choice of an effective origin is additionally unnecessary. In this respect, the comparison of predicted and measured skin friction is the most unambiguous test which can be made.

An excellent set of experimental data for this purpose is presented by Hopkins, et al (Ref. 3) for a flat plate. Unfortunately, the wall enthalpy ratio does not extend down to the range of interest but the Mach numbers and Reynolds numbers are in the correct range. Following the approach of Ref. 3, the comparison is given in terms of

$$\frac{c_{f(exp)} - c_{f(calc)}}{c_{f(exp)}} \times 100$$

which gives a percent relative error. The calculated values are determined for the same Mach number, Reynolds number, and wall enthalpy ratio as the individual experimental points to which they are compared. The comparison is shown on Fig. 1 as a function of the wall enthalpy ratio but there is no strong indication of any dependence of the error on the wall enthalpy ratio. It is indicated, however, that the error is slightly less for the lower Mach number. The error was also plotted against the momentum thickness Reynolds number, but there was no indication of a dependence of the error on this parameter and the curve is not shown. This set of data allows a rather clear distinction between the accuracy of each method. The two most accurate predictions are given by Eckert's and Spalding and Chi's methods which is easily seen from the spread of errors summarized in the following table.

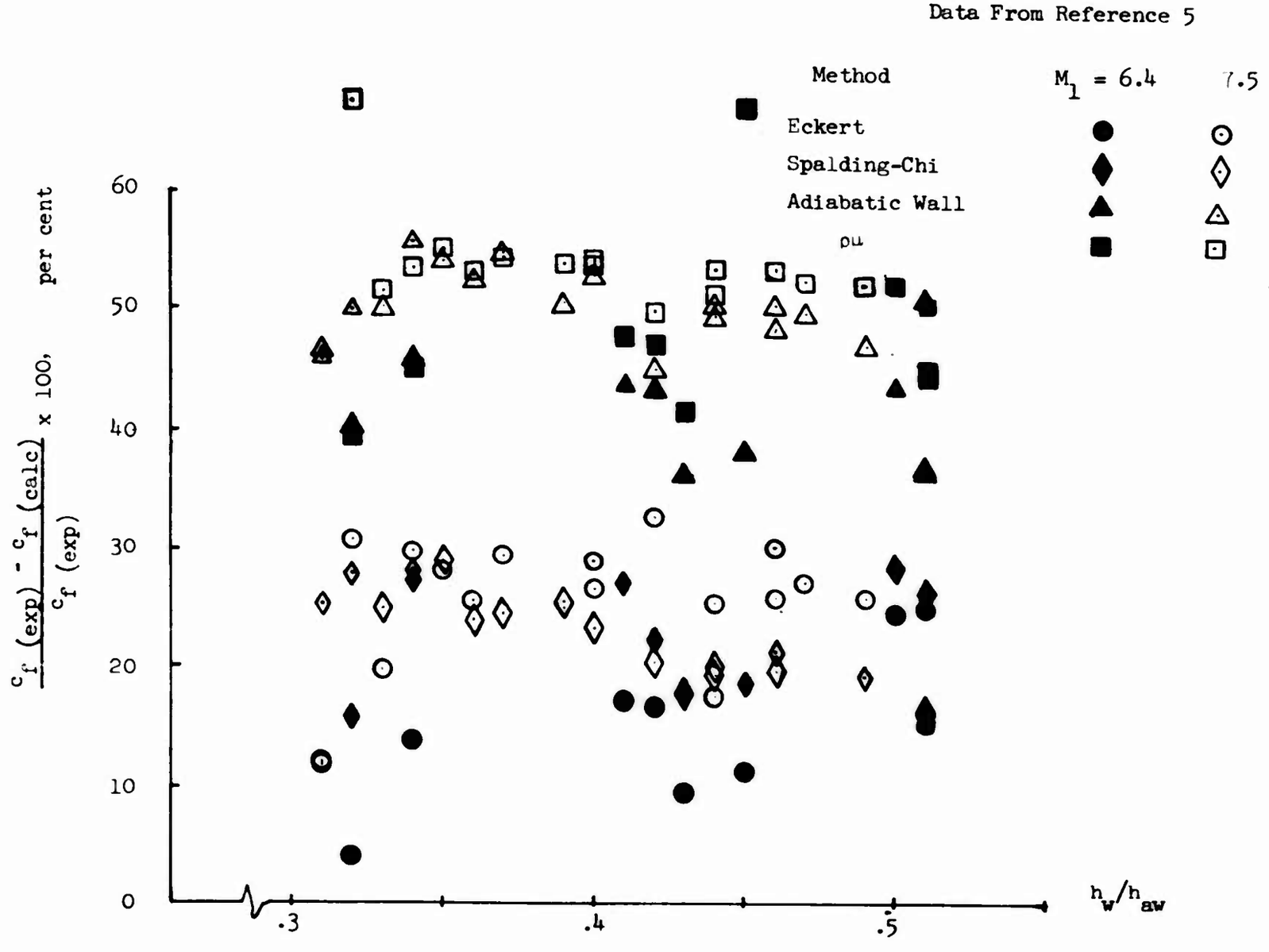

Figure 1. Comparison of Measured and Calculated Skin Friction

Table 5. Range of Relative Errors in the Comparison with Skin Friction Data from Ref. 3 (error in %)

Method	$M_1 = 6.5$	$M_1 = 7.4$
Eckert	4-25	12-33
Spalding-Chi	16-28	19-28
Adiabatic Wall	36-51	45-56
$(\rho\mu)$	39-52	45-55

Errors given by the adiabatic wall reference enthalpy and the $\rho\mu$-method are nearly twice as large as the other two. In addition to the relative accuracy of each prediction, it is important to notice that each method consistently underpredicts the skin friction (positive error).

A comparison of the predictions from Eckert's method and the Spalding-Chi method was made in Spalding and Chi's original paper (Ref. 11). That comparison was made separately for data with and without heat transfer and is summarized in the following table. (Spalding and Chi define their error as $[c_{f(exp)} - c_{f(calc)}]/c_{f(calc)}$.)

Table 6. Comparison with Skin Friction Data Made by Spalding and Chi in Ref. 11 (error, percent, root-mean-square).

Method	Without heat transfer	With heat transfer	Over-all error
Spalding-Chi	8.6	12.5	9.9
Eckert	12.2	20.2	15.1

The set of data used in the comparison was very extensive but did not include wall enthalpy ratios as small as those of interest for the STS orbiter.

An indication of the effect of Mach number on the accuracy of the predictions is given in Fig. 2. The data is that which is summarized in Ref. 4 and is for an adiabatic wall and is used here only because it covers the appropriate Mach number range. It should be noted that for an adiabatic wall, the Eckert and adiabatic wall reference enthalpies are the same. As the Mach number decreases the predictions all become of comparable accuracy, and in contrast to the comparison in Fig. 1, the methods give both positive and negative errors, which are within ±15 percent for a Mach number less than 5. An error of this magnitude is probably comparable to the errors in the skin friction laws themselves. At the highest Mach number, each method gives only a positive error, in agreement with the comparison in Fig. 1.

Skin friction data at wall enthalpy ratios near the range of interest but at Reynolds numbers generally a little larger than those of primary interest were measured by Wallace and McLaughlin (Ref. 5). The comparison is given in Fig. 3 for the three runs with the lowest wall enthalpy ratios. A summary of the range of errors is given in the following table.

Table 7. Range of Relative Errors in the Comparison with Skin Friction Data from Ref. 5 (error in %)

	h_w/h_{aw} = 0.142	0.143	0.139
Method	M_1 = 5.56	6.67	7.4
Eckert	-24.1 to 9.8	-15.7 to 0.8	-28.2 to 3.3
Spalding-Chi	-9.7 to 19.3	-5.1 to 13.2	-12.5 to 18.8
Adiabatic wall	26.2 to 46.4	29.5 to 41.7	25.3 to 43.6
($\rho\mu$)	9.8 to 39.3	17.1 to 30.5	10.6 to 32.4

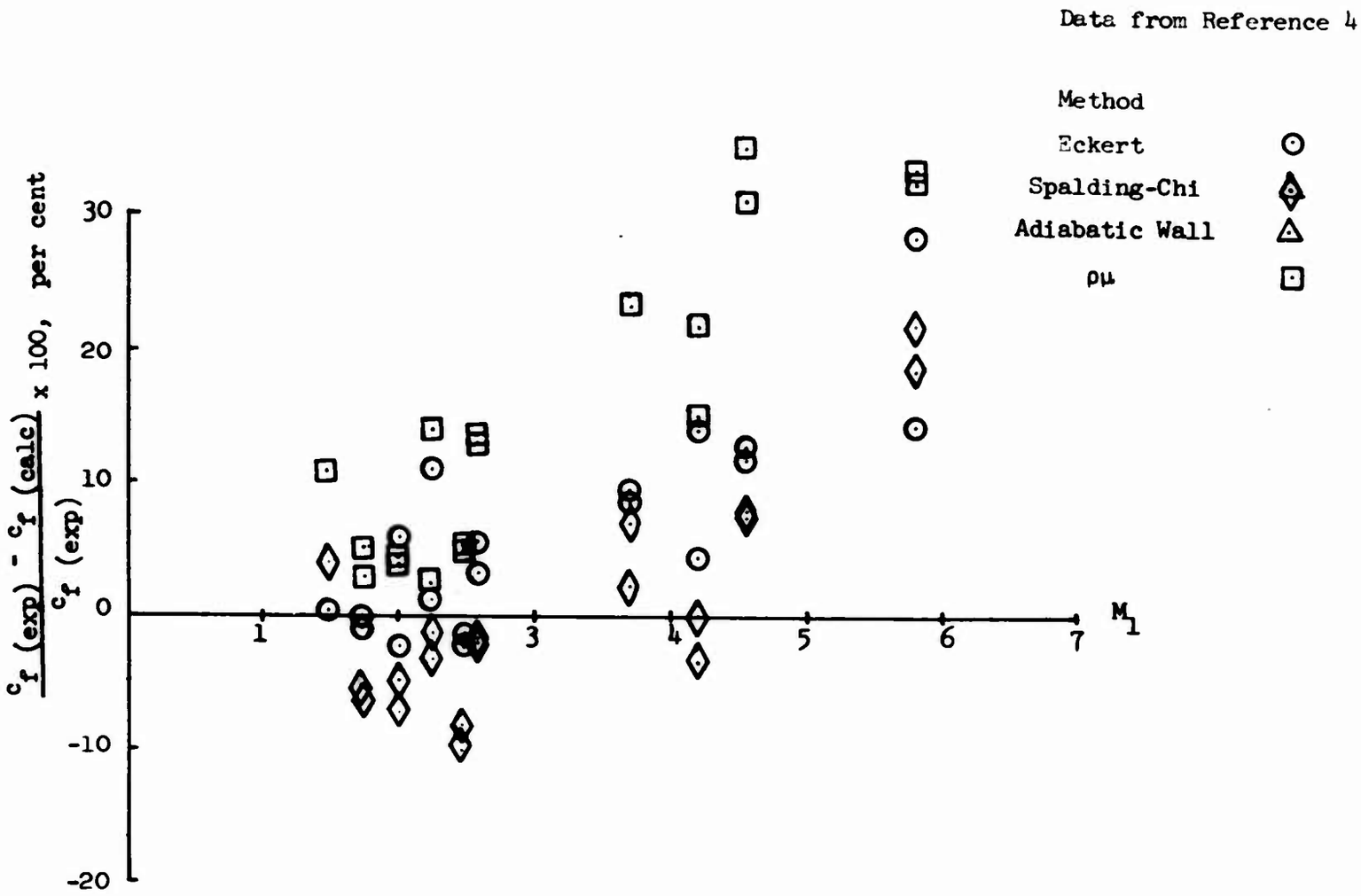

Figure 2. Comparison of Measured and Calculated Skin Friction on an Adiabatic Wall

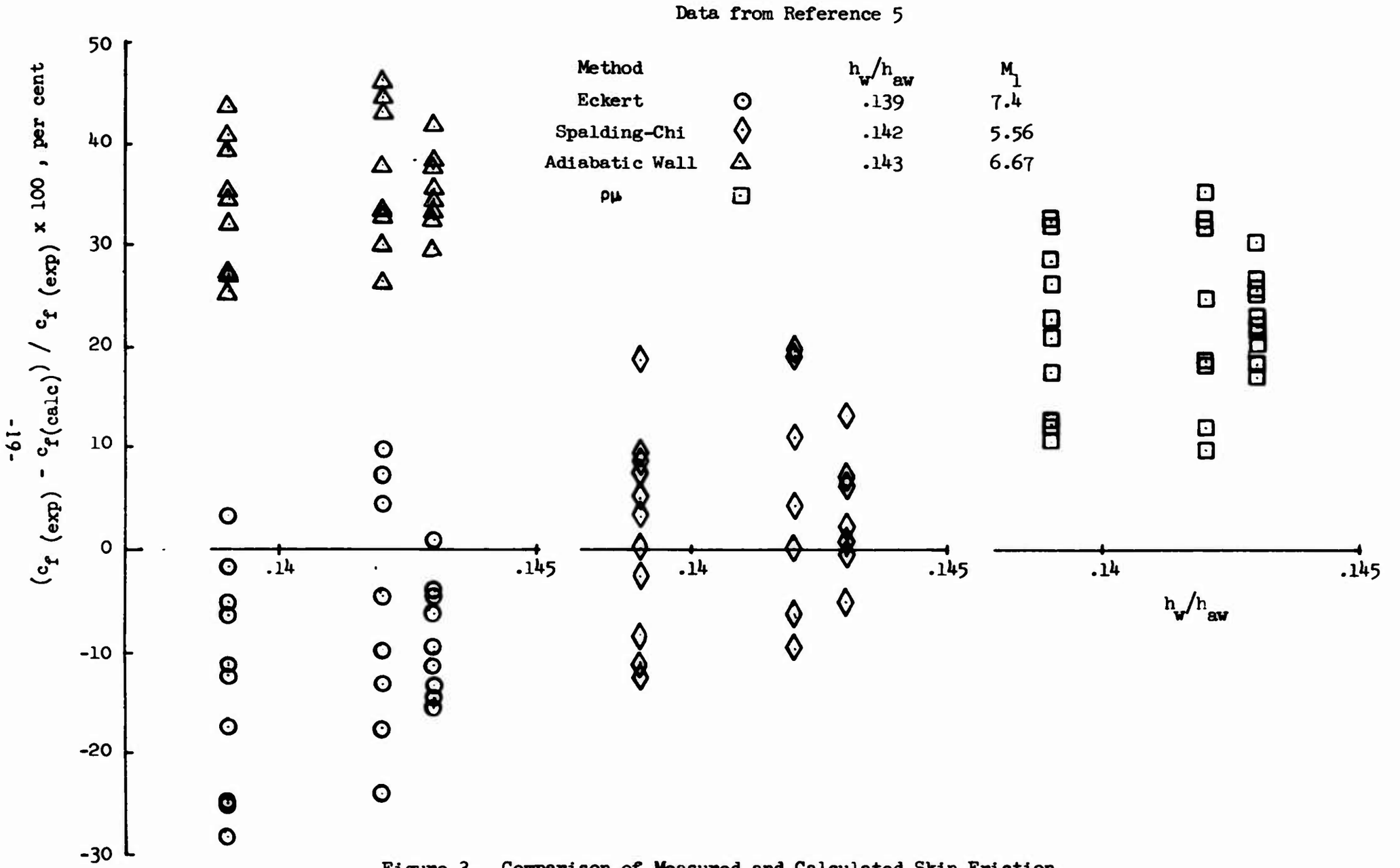

Figure 3. Comparison of Measured and Calculated Skin Friction

The results of this comparison are like those shown in Table 5 for the data from Ref. 3. Each set of data shows the Eckert and the Spalding-Chi methods give the best estimates of the four methods tested. In this case, however, where the wall enthalpy ratios are smaller than those in the data from Ref. 3, both Eckert's and Spalding and Chi's predictions give both positive and negative errors. It is not possible to determine if this is an effect of the wall temperature ratio or if it is an indication of more scatter in the experimental data. For these conditions, however, the comparison does allow a clear distinction of the relative accuracy of the predictions from each method.

To briefly summarize this section containing the skin friction comparison, the data used here clearly indicates that the Eckert and Spalding-Chi methods give estimates of the skin friction which are superior to those obtained from the adiabatic wall reference enthalpy and $(\rho\mu)$-methods. In general, the predictions from Eckert's method are slightly larger than those from Spalding and Chi's. Without additional data, particularly at lower wall enthalpy ratios, it is not possible to make a finer distinction between the predictions of these two methods.

VII. REYNOLDS ANALOGY

Reynolds analogy is used to obtain the heat transfer from skin friction estimates. The two expressions for the analogy factor used with the four methods tested here are either the Colburn equation or the Von Karman equation based on the Prandtl number and skin friction coefficient in the equivalent incompressible flow. The approach to selecting the appropriate analogy factor in this report is to examine some measurements of the analogy factor in order to determine the most appropriate value. Direct measurements are reported by Hopkins, et al (Ref. 3) and Wallace and McLaughlin (Ref. 5). These data are compared with the predictions from both the Colburn and Von Karman equations in Fig. 4. The arithmetic average of each set of experimental data is summarized in the following table.

Table 8. Average Reynolds Analogy Factors from Ref. 5

	h_w/h_{aw} = 0.142	0.143	0.139
	M_1 = 5.6	6.67	7.4
$(2\,St/c_f)_{avg}$	1.00	1.126	1.065

The skin friction is transformed according to the Spalding and Chi method in order to make the results of Ref. 5 comparable to those from Ref. 3. It is suggested by this comparison that the expression which is most representative of the true analogy factor for the data shown here is Von Karman's equation and the majority of the data clearly indicates that Colburn's equation predicts too large an analogy factor.

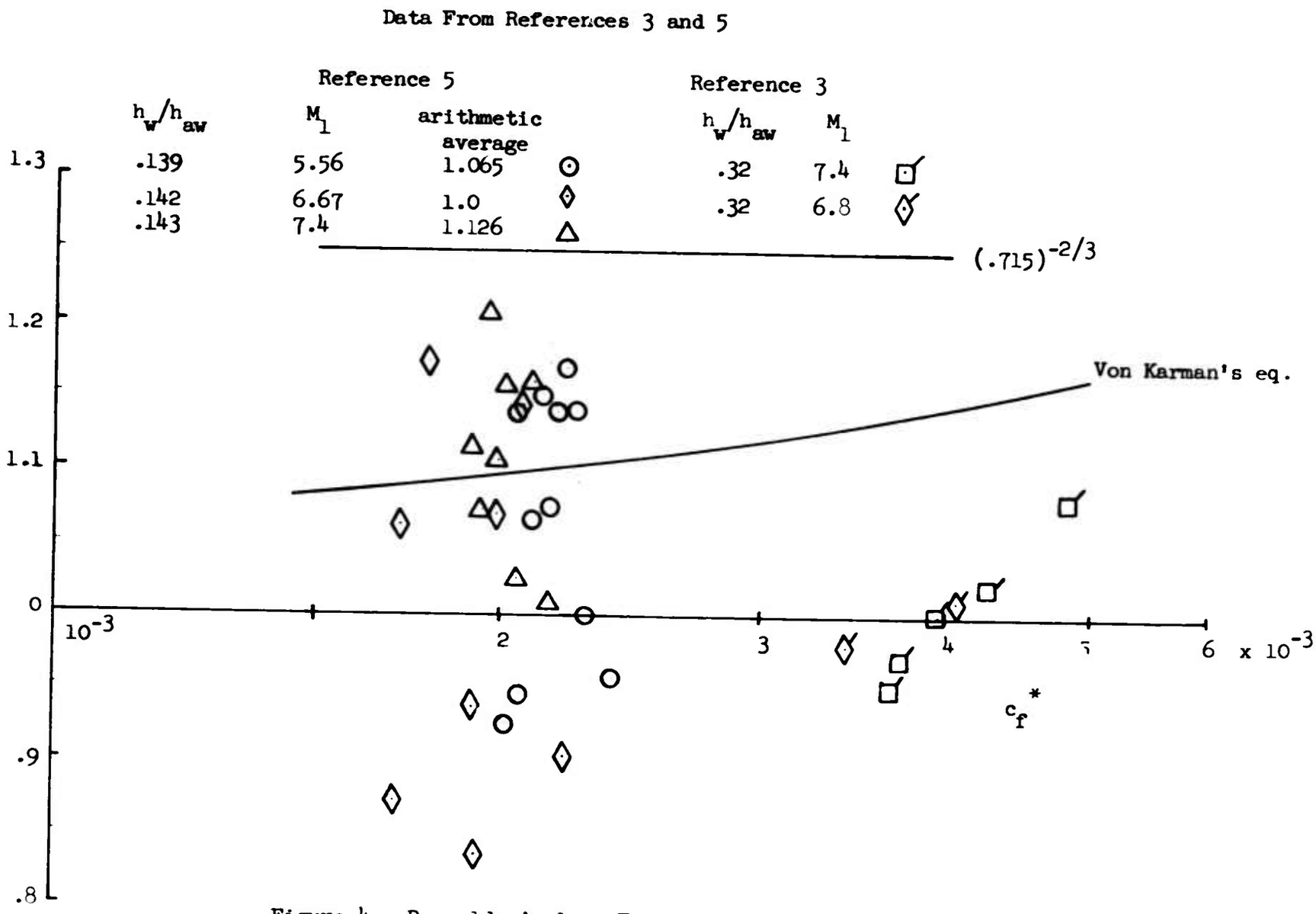

Figure 4. Reynolds Analogy Factor

A choice of the Reynolds analogy factor to be used in a heat transfer calculation is independent of the particular method although a particular form of the analogy factor is usually associated with one method. For example, Eckert's, the adiabatic wall reference enthalpy, and the $(\rho\mu)$-methods are usually used with the Colburn equation and Spalding and Chi's method has been used with the Von Karman equation. For the subsequent predictions of heat transfer in this report, Von Karman's equation will be used with Eckert's method and Spalding and Chi's method and Colburn's equation will be used with the other two methods. These are the particular combinations of analogy factor and heating prediction method which give the best estimates of heating for a particular method without extending the analogy factor beyond those values predicted by either of these two equations. In the subsequent calculations, Von Karman's equation is based on the transformed skin friction c_f^*, and a constant Prandtl number of 0.715 is used. In the $(\rho\mu)$-method, the analogy factor of $\sigma^{*-0.645}$ is used instead of $\sigma^{*-2/3}$, following the description of the method (Ref. 8).

VIII. COMPARISON WITH HEAT TRANSFER DATA

As mentioned previously, there are published comparisons of heat transfer predictions which include some of the methods used here. In particular, the two reviews (Refs. 1 and 2) compare Spalding and Chi's method with Eckert's and with Eckert's and the $\rho\mu$-method, respectively. In both comparisons the Spalding-Chi method was found to give the most consistently accurate predictions of those methods tested.

The heat transfer data reported by Wallace and McLaughlin (Ref. 5) has been used in some of the previous comparisons. The comparison is repeated here in the same form as the comparison of the skin friction. That is, a relative error

$$\frac{St_{exp} - St_{calc}}{St_{exp}} \times 100$$

is computed for each data point. In the present comparison, only the data at the lowest wall enthalpy ratios are considered. These ratios are almost within the range of interest and the Mach numbers are in the appropriate range. However, the Reynolds numbers are generally larger than those of primary interest. Heat transfer rates at the lower wall enthalpy ratios are compared with the estimated values in Fig. 5. In agreement with the previous work, the Spalding and Chi prediction along with Von Karman's equation for the analogy factor gives the most accurate predictions. Eckert's method with the Von Karman equation overpredicts the heat transfer with about the same error as the $\rho\mu$-method, with Colburn's equation, underpredicts it. The adiabatic wall reference enthalpy method, even with the Colburn equation, predicts heat transfer rates that are from 10 to 35 percent too low. The range of the errors in this comparison are summarized in Table 9.

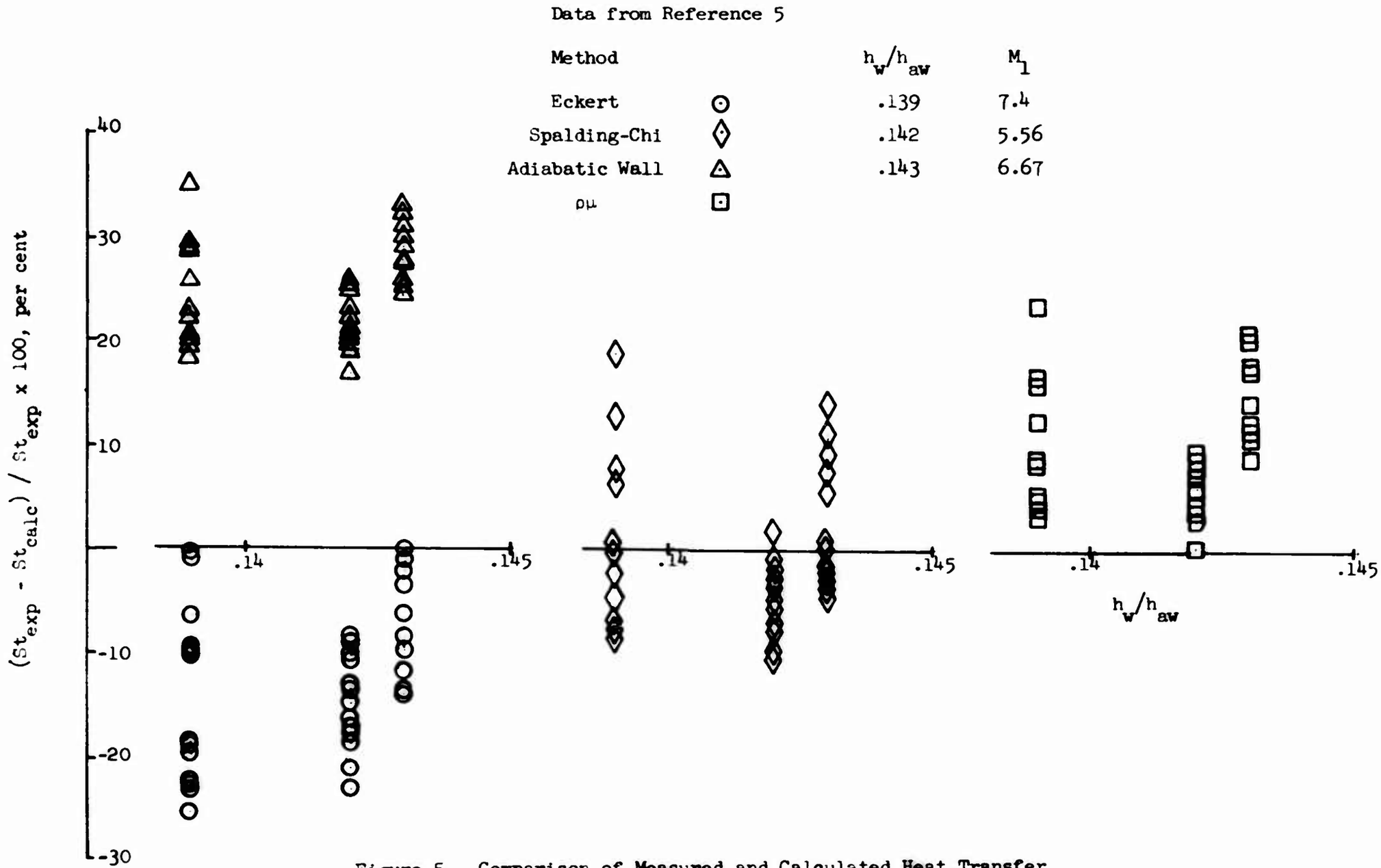

Figure 5. Comparison of Measured and Calculated Heat Transfer

Table 9. Range of Relative Errors in the Comparison with Heat Transfer Data from Ref. 5 (error in %)

		h_w/h_{aw} = 0.142	0.143	0.139
Method	**Analogy Factor**	M_1 = 5.56	6.67	7.4
Eckert	**Von Karman**	-23.4 to -8.6	-13.9 to -1.1	-25.4 to -0.7
Spalding-Chi	**Von Karman**	-11.1 to -1.7	-4.3 to 14.0	-9.1 to 18.7
Adiabatic Wall	**Colburn**	16.8 to 25.8	24.9 to 33.6	8.5 to 35.4
($\rho\mu$)	**Colburn**	0.2 to 9.6	9.1 to 21.4	3.0 to 23.4

By comparing the errors in the skin friction comparison summarized in Table 7 with the above summary for heat transfer it can be seen that the magnitudes are about the same for the Eckert and Spalding and Chi methods while the error in the heat transfer is less than that in the skin friction for the ($\rho\mu$) and adiabatic wall reference enthalpy methods. This can be traced to the Reynolds analogy factor used for each method. Von Karman's equation, which gives values near the average of the measured analogy factors is used with Eckert's and Spalding and Chi's methods and therefore the error in the skin friction and heat transfer are nearly the same. In contrast, the Colburn equation gives values from 15 to 20 percent greater than the measurements and consequently compensates for some of the error in the skin friction predictions for the ($\rho\mu$) and adiabatic wall reference enthalpy methods.

It is possible to compensate entirely for the error in any of the methods by defining an "effective" analogy factor different from that given by either of the two equations used here. For Eckert's method, an analogy factor of unity would partially correct for the tendency of this method to overpredict the heat transfer for these conditions. The ($\rho\mu$)-method and the adiabatic wall reference enthalpy would require analogy factors of about 1.35 and 1.45, respectively, to resolve most of the error in the heat transfer predictions. Only Spalding and Chi's method gives nearly correct estimates of the skin friction and also of the heat transfer when using the Von Karman equation, which essentially agrees with the measured values of the analogy factor. For these reasons, the Spalding and Chi method is indicated to be the most accurate based on the comparison with this set of experimental data.

The only source of data at lower wall enthalpy ratios was found to be from measurements in shock tubes on the inside surface of circular cylinders. Measurements reported by Hopkins and Nerem (Ref. 6) and by Jones (Ref. 7) are considered for this report. Since the measurements were not made on flat plates, although that is the shape the experiments were designed to simulate, the effects of non-uniform boundary layer edge conditions, reflected shocks, and transverse curvature are unknown factors in the data. An

indication of the importance of transverse curvature can be obtained by comparing the approximate boundary layer displacement thickness with the tube radius for the two experiments. This is done in the following table for the displacement thickness at the heat transfer gage furthest from the leading edge.

Table 10. Displacement Thicknesses on the Inside of the Tube Wall

Reference	Tube Radius, cm	δ^*/R
(6)	2.54	0.1
(7)	2.2	0.45

Curvature effects are expected to be less in the data from Ref. 6, but as a consequence of taking data so near the leading edge, a boundary layer trip was needed to assure fully turbulent flow.

The data of Hopkins and Nerem (Ref. 6) is of interest because of the low wall enthalpy ratio; the values of 0.012 - 0.026 are even smaller than the lowest values in the range of interest for the STS. The comparison is included here in order to provide an end point to which the accuracy of each calculation method can be extrapolated across the whole wall enthalpy range of interest. The errors for each method were computed but only the errors for Spalding and Chi's method and the adiabatic wall reference enthalpy are shown in Fig. 6. The other two methods gave predictions that were 100 percent or more too large. For this set of data, the Spalding and Chi method with Von Karman's equation for the analogy factor is the only one of the four methods to give a reasonable estimate of the heat transfer. Moreover, even though the data is questionable because of the test surface geometry and boundary layer trip, it strongly suggests that Spalding and Chi's method gives the most correct dependence of the heating on the wall enthalpy ratio.

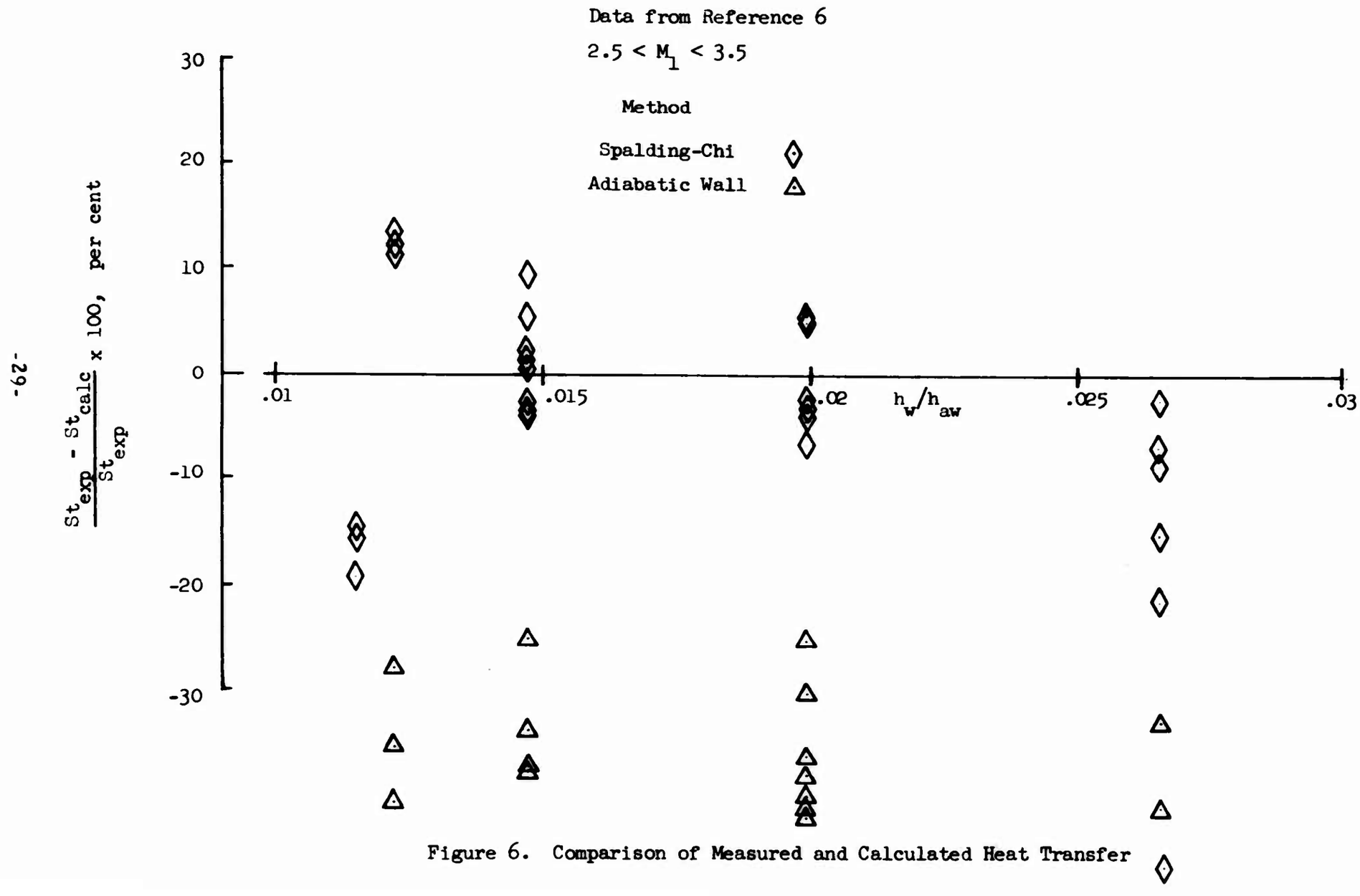

Figure 6. Comparison of Measured and Calculated Heat Transfer

In addition to the low wall enthalpy ratios, the data from Ref. 6 is the only set so far which requires that real gas effects be taken into account. The stagnation enthalpy for these data is comparable to that of actual reentry conditions. As a consequence of this and the low wall enthalpy ratios, it is important to note that the relative ordering of the amount of heat transfer predicted by each method is different from that of the conditions for the wind tunnel data. For ordinary wind tunnel conditions, the heat transfer predictions are largest for Eckert's method, then followed by Spalding and Chi, then the $\rho\mu$-method, and the adiabatic wall reference enthalpy method gives the smallest estimates. For the conditions of the tests of Ref. 6, the Eckert and $\rho\mu$-methods give the largest estimates, with Eckert's method giving a slightly higher estimate than the $\rho\mu$-method. The adiabatic wall reference enthalpy method gives the next lowest estimate, and finally the Spalding and Chi method gives the lowest. There is more than a factor of two difference between the Eckert and Spalding and Chi estimates. The effect of wall enthalpy ratio and perhaps also Mach number is therefore seen to be very important at the lower end of the range of interest for the STS. These conditions occur for the higher angles of attack, say more than 40 deg.

The data obtained by Jones (Ref. 7) coincides with the wall enthalpy ratio and Reynolds number range of interest. Because of the large ratio of displacement thickness to radius, however, its validity in approximating the conditions on a flat plate is questionable. It is included in the present comparison only because it is the only set of data which matched the precise values of the wall enthalpy ratios which are of primary interest. It also requires that real gas properties be used. The comparison is made in Fig. 7. For this data, the Eckert and $\rho\mu$-methods give the best predictions, with Spalding and Chi's and the adiabatic wall reference enthalpy methods generally underpredicting the heat transfer.

Since the scatter in this data is large, the results of the comparison are summarized in the following table by giving the percent of the predictions that fall within ± 15 percent of the data, rather than indicating the spread of the error.

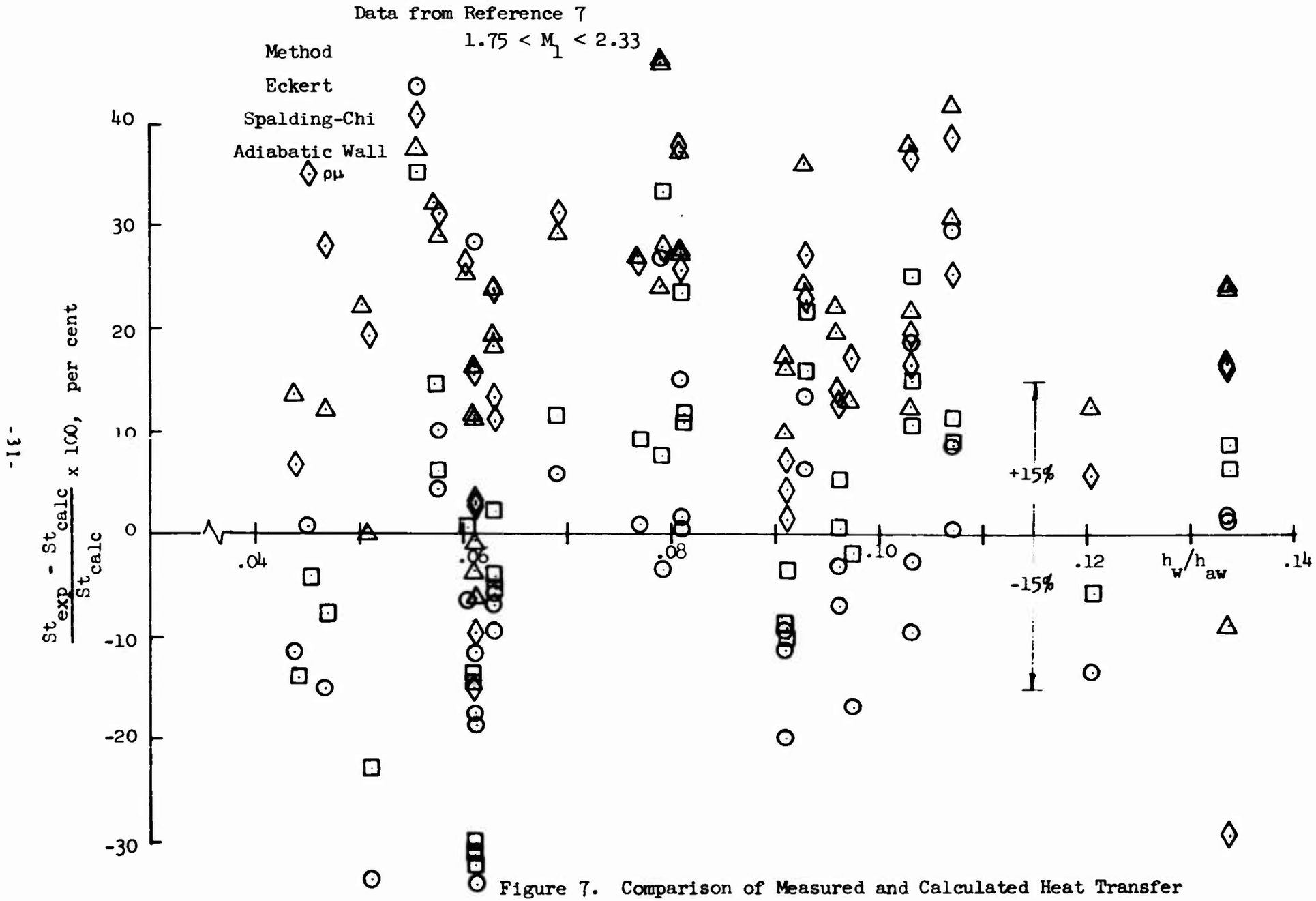

Figure 7. Comparison of Measured and Calculated Heat Transfer

Table 11. Percent of the Predictions Which Give Relative Errors Within ±15 Percent of the Heat Transfer Data from Ref. 7

Method	Analogy factor	Percent Within ±15 Percent
Eckert	Von Karman	71.0
Spalding-Chi	Von Karman	34.2
Adiabatic Wall	Colburn	29.3
$\rho\mu$	Colburn	68.3

This comparison yields results which are contradictory to those from the comparison with Hopkins and Nerem's data. The only indication of which conclusion should be weighted the most heavily is the relative importance of transverse curvature, which, according to Table 10, should have a larger effect on the data from Jones' work (Ref. 7) than in that from Hopkins and Nerem (Ref. 6). Therefore, it is reasoned here that Spalding and Chi's method still is indicated to give the best estimate of heat transfer for the conditions applicable to the STS orbiter.

An additional source of data for the heat transfer in the correct Mach number and Reynolds number range is the extensive measurements made on the X-15 aircraft. The wall enthalpy ratios are larger than those of interest for the STS. This data was examined in the preparation of this report and, as previously indicated (Refs. 8 and 10), the adiabatic wall reference enthalpy and $\rho\mu$-methods gave the best estimates. However, it is argued here that the X-15 data, aside from the fact that the wall enthalpy ratio is beyond the range of present interest, is less appropriate than the wind tunnel data for the purpose of distinguishing the accuracy of one method from another. This is because the flight test data includes the effect of a nonuniform free stream because the test surfaces were within the conical flow field of the body. In addition, there were pressure gradients along the test surfaces and the wall temperatures were nonuniform. There is also the

uncertainty concerning the initiation of turbulent flow due to surface discontinuities. For these reasons, the wind tunnel data used here, which is essentially free from these effects, is weighed more heavily in the present comparison. And, the wind tunnel data supports the choice of Spalding and Chi's method with the Von Karman analogy factor as that prediction method which most accurately accounts for the effect of the density and transport property variation through the turbulent boundary layer on a smooth flat plate for the range of Mach number, Reynolds number, and wall enthalpy ratio applicable to the STS orbiter.

IX. EFFECTIVE ORIGIN OF TURBULENT FLOW

A discussion of the choice of a virtual origin is included with this comparison of calculation methods because the error in using the leading edge rather than a more realistic origin for the turbulent boundary layer is comparable to the difference in the heating predicted by the different methods. This is particularly true for the STS orbiter, where transition and fully turbulent flow can occur far back on the vehicle at the peak heating conditions. It is the objective of this section to compare the heat transfer predictions using several definitions of an effective origin with experimental data for heating at the onset of fully turbulent flow. This comparison is not made to carefully select the most appropriate definition of the effective origin but only to illustrate that the heating in the initial region of fully turbulent flow can be approximated by simply redefining the length used in the heat transfer estimates used in this report.

It was suggested by Dhawan and Narasimha (Ref. 13) that the effective origin of the turbulent boundary layer is near the point of transition onset when the transition region is of finite length. When transition is taken to be abrupt, Reynolds, Kays, and Kline (Ref. 14) propose that the laminar and turbulent boundary layer momentum thickness should be matched at the transition point. This model is also applicable to a gradual transition if the point of matching is taken to occur in the transition region at, say, the point midway between onset and fully turbulent flow. The data presented in Ref. 1 was examined on the basis of the effective origin being at the point of maximum heating. This definition is not useful for the purpose of this report, however, because it is the maximum heating itself which is the most important quantity. An alternative which gives nearly the same results and is claimed by Henderson (Ref. 15) as being the point which provides the most consistent correlation of the data is an origin at a point about 20 percent of the transition region length upstream from the point of fully turbulent flow. Three of these definitions are utilized and the results are compared with experimental data.

Two sets of data are used for the comparison and the results are given in Figs. 8 and 9 where both Eckert's and the Spalding and Chi predictions are shown. The Eckert prediction is corrected by defining an effective origin at transition onset and also at a point 80 percent of the distance between onset and fully turbulent flow. The third correction uses a momentum thickness match at halfway through the transition region. Also, Spalding and Chi's predictions are corrected by using an effective origin at 80 percent of the transition region length, which is the combination of heating method and definition of effective origin recommended by Henderson (Ref. 15). In both cases, the most accurate prediction is given by Eckert's method with the effective origin given by matching momentum thicknesses at a point halfway between transition onset and fully turbulent flow. The effective origin at the onset of transition gives nearly the correct heating estimates, so either of these two definitions appear to give satisfactory definitions of the effective origin. The effective origin near the end of transition gives inferior heating predictions when used with either Eckert's or Spalding and Chi's method.

Curve	Method	Origin
1	Eckert	Leading Edge
2	"	Onset, $Re_x = 4 \times 10^6$
3	"	Momentum Matching at $Re_x = 6.5 \times 10^6$
4	"	80 per cent of Transition Region; $Re_x = 5 \times 10^6$
5	Spalding-Chi	Leading Edge
6	"	80 per cent of Transition Region

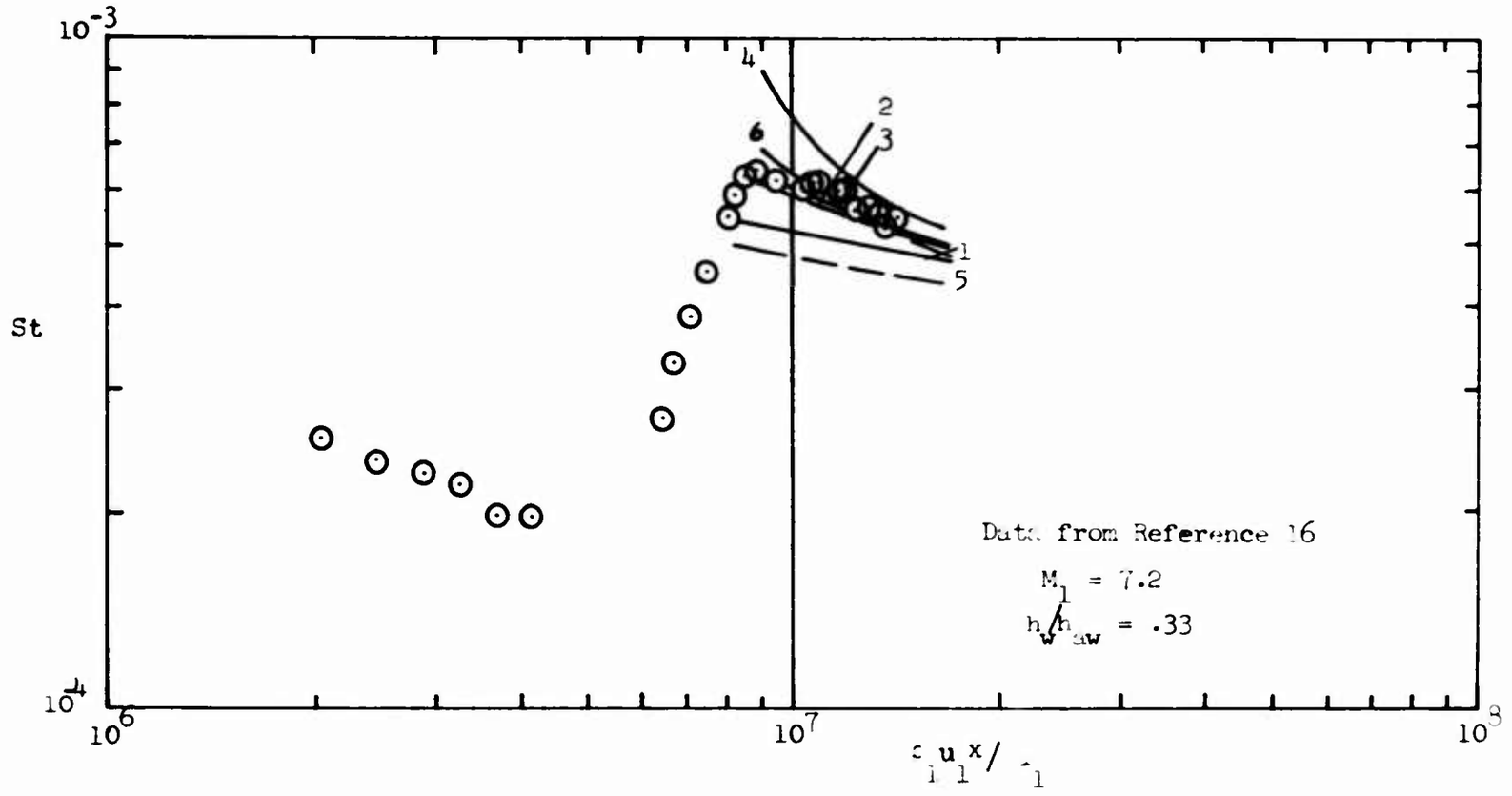

Figure 3. Comparisons of Different Effective Origins for the Turbulent Boundary Layer

Curve	Method	Origin
1	Eckert	Leading Edge
2	"	Onset, $Re_x = 7.2 \times 10^6$
3	"	Momentum Matching at $Re_x = 1.1 \times 10^7$
4	"	80 per cent of Transition Region, $Re_x = 1.34 \times 10^7$
5	Spalding-Chi	Leading Edge
6	"	80 per cent of Transition Region

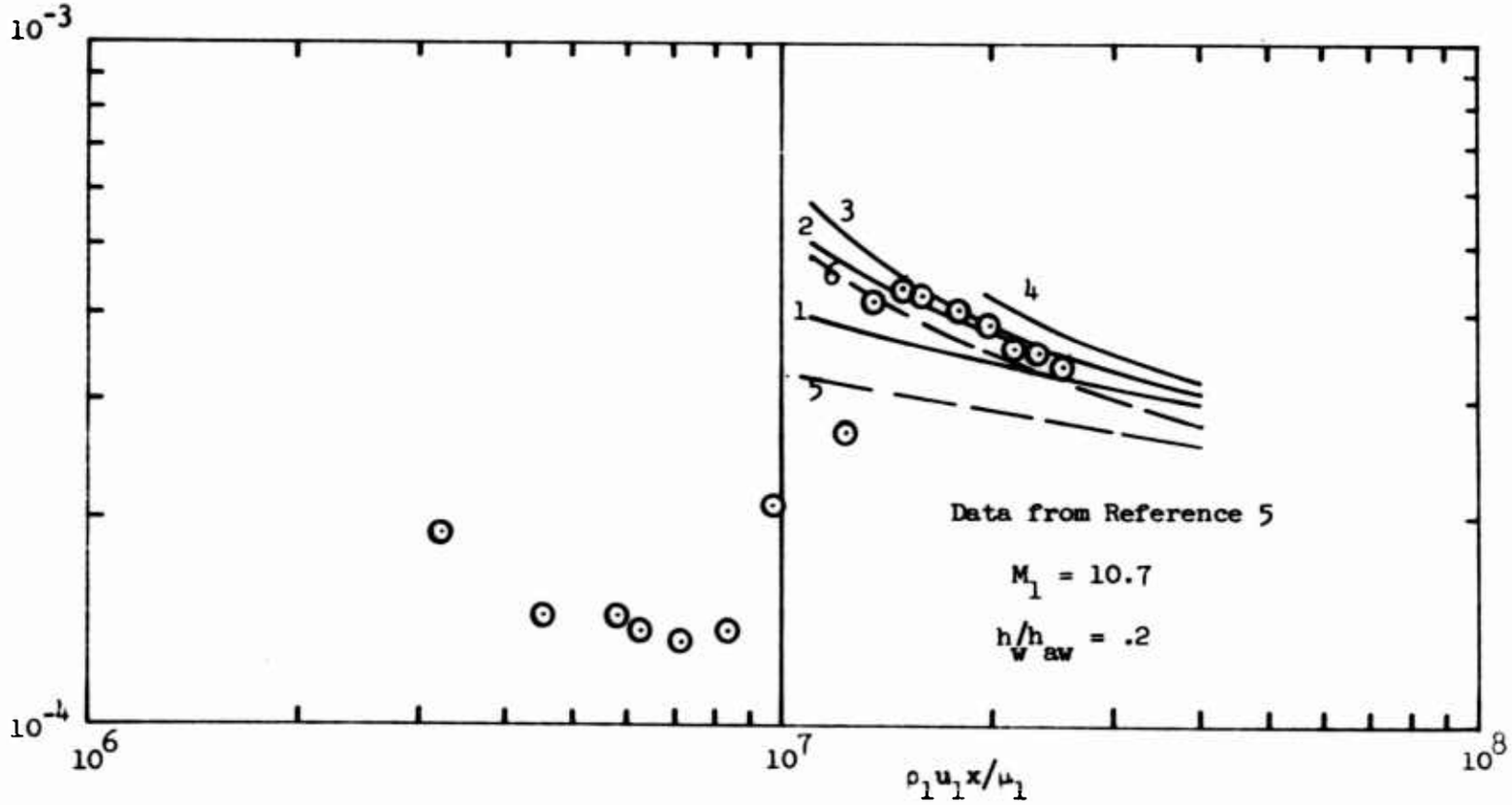

Figure 9. Comparison of Different Effective Origins for the Turbulent Boundary Layer

X. SUMMARY AND CONCLUSIONS

Four procedures for calculating the heat transfer through a turbulent boundary layer have been examined and are shown to be different adaptations of the same basic approach. The procedures are all based on transforming a compressible turbulent flow to an equivalent incompressible flow where the density and viscosity are evaluated at some mean state of the fluid. The essential differences between the methods are due to the different reference enthalpies at which the properties are evaluated and the different factors which multiply the skin friction coefficient and Reynolds number in the compressible flow to give the equivalent incompressible flow. Each of the methods examined is strictly applicable to flow over a smooth flat plate.

A comparison of the predictions of the skin friction with experimental data shows that each method tends to underpredict the skin friction coefficient. The most consistently accurate predictions are given by the Spalding and Chi method, although the relative errors from this prediction can be from -12.5 to 28 percent. The next most accurate method is Eckert's, with errors between -28 and 33 percent, and then the $\rho\mu$-method, with errors between 10 and 55 percent. The adiabatic wall reference enthalpy method was the most unsatisfactory; consistently underpredicting the data with errors between 25 and 56 percent.

Direct measurements of Reynolds analogy factor indicate that the correct value for the compressible turbulent boundary layer on a flat plate at conditions approximating those of the STS orbiter bottom surface should be between about 1 and 1.12. Von Karman's equation gives values that are near the correct value and Colburn's equation predicts values about 20 percent too large.

A comparison of the predictions by each method with experimental heat transfer data shows that the most consistently accurate estimates of the heat transfer to a smooth flat plate with boundary layer edge conditions approximating those of the STS orbiter are given by Spalding and Chi's method with

Von Karman's equation for the analogy factor. For the data used in the comparison, the errors are generally in the range of ±20 percent. Predictions from Eckert's method with Von Karman's analogy factor and the $\rho\mu$-method with the Colburn equation give errors which are of comparable magnitude, with those from Eckert's method generally overpredicting the data and those from the $\rho\mu$-method underpredicting the data, except at very low wall enthalpy ratios. The adiabatic wall reference enthalpy method with Colburn's equation consistently underpredicts the heating by about 15 percent or more, except at the very low wall enthalpy ratios.

Several definitions of the effective origin for the turbulent boundary layer were tested by comparison with experimental data involving transitional heating. For the limited comparison given here, the effective origin defined by matching the laminar and turbulent momentum thicknesses at a point halfway between transition onset and fully turbulent flow gives the best agreement. An effective origin at the point of transition onset gives nearly as good an estimate. Both definitions provide improved estimates of the heating in the initial region of fully turbulent flow.

The above conclusion that Spalding and Chi's method gives the best estimate of the heat transfer must be qualified by the fact that only a very limited amount of data was available for comparison. Moreover, not all of this data is free from uncertainty. More importantly, this conclusion is only applicable to heating estimates for a smooth flat plate with no longitudinal or transverse pressure gradients and therefore the estimates only account for the effects of variable density and transport properties. An extension of this conclusion to say that the Spalding and Chi method will give the best estimates of the actual heating on the STS orbiter can only be made when it is determined that the boundary layer on the bottom surface is indeed closely approximated by that over a smooth flat plate with no pressure gradients.

There is no real assurance that the boundary layer on the windward surface of a large lifting reentry vehicle can be approximated by that on a flat plate. An obvious example of the limitations of this approximation is

available from the data on the X-15 aircraft. Flight test data supports the choice of the adiabatic wall reference enthalpy method as the most accurate prediction while the wind tunnel data suggests that this method gives the poorest predictions. It must be concluded from this contradiction that there are other factors such as pressure gradients, wall temperature gradients and boundary layer trips whose effects are comparable to that of the variable properties and density. Extending this example to the STS orbiter, the uncertainties about the nature of the actual boundary layer on a vehicle in flight suggests that for design purposes an adequate margin of safety should be assigned to the estimates of the heating.

NOMENCLATURE

Symbol	Meaning	Dimensions
$c_f = \tau_w/\rho_1 u_1^2$	local skin friction coefficient	
$c_f^* = \tau_w/\rho^* u_1^2$	transformed skin friction coefficient	
F_{Rx}	Length Reynolds number multiplication factor	
$F_{R\theta}$	Momentum thickness Reynolds number multiplication factor	
F_c	Skin Friction coefficient multiplication factor	
h	Enthalpy	Btu/lb
k	Reynolds analog factor, $2St/c_f$	
M	Mach number	
q	heat flux	Btu/ft^2-sec
$Re_x = \rho_1 u_1 x/\mu_1$	Reynolds number	
$Re_x^* = \rho^* u_1 x/\mu^*$	Transformed Reynolds number	
$Re_\theta = \rho_1 u_1 \theta/\mu_1$	Momentum thickness Reynolds number	
$Re_\theta^* = \rho^* u_1 \theta^*/\mu^*$	Transformed momentum thickness Reynolds number	
r	Recovery factor	
$St = q/\rho_1 u_1 (h_{aw}-h_w)$	Stanton number	

NOMENCLATURE (Continued)

Symbol	Meaning	Dimensions
$St^* = q/\rho^* u_1 (h_{aw} - h_w)$	Transformed Stanton number	
u	velocity	ft/sec
x	length	ft
ρ	density	lb/ft^3
μ	viscosity	lb/ft-sec
σ	Prandtl number	
τ	Shear stress	lb/ft^2
θ	Momentum thickness	ft

Subscripts

1	boundary layer edge
aw	adiabatic wall
w	wall
o	stagnation

Note: the superscript * indicates a quantity for the uniform property flow evaluated at the reference enthalpy.

REFERENCES

1. Bertram, M. H., and L. Neal, Jr., "Recent Experiments in Hypersonic Turbulent Boundary Layers," AGARD Specialists Meeting on Recent Development in Boundary-Layer Research, Naples (1965), also NASA TM-X-56335.

2. Bertram, Cary, A. M., Jr., and A. H. Whitehead, "Experiments with Hypersonic Turbulent Boundary Layers on Flat Plates and Delta Wings," AGARD Specialists Meeting on Hypersonic Boundary Layers and Flow Fields, London (1968).

3. Hopkins, E. J., et al, "Summary and Correlation of Skin-Friction and Heat-Transfer Data for a Hypersonic Turbulent Boundary Layer on Simple Shapes," NASA TN D-5089 (1969).

4. Peterson, J. B., Jr., "A Comparison of Experimental and Theoretical Results for the Compressible Turbulent-Boundary-Layer Skin Friction with Zero Pressure Gradient," NASA TN-D-1795 (1963).

5. Wallace, J. E., and E. J. McLaughlin, "Experimental Investigation of Hypersonic Turbulent Flow and Laminar, Lee-Side Flow on Flat Plates," AFFDL-TR-66-63, Vol. 1 (1966).

6. Hopkins, R. A., and R. M. Nerem, "An Experimental Investigation of Heat Transfer from a Highly Cooled Turbulent Boundary Layer," AIAA Journal 6 (10), pp. 1912-1918 (1968).

7. Jones, J. J., "Shock-Tube Heat-Transfer Measurements on Inner Surface of a Cylinder (Simulating a Flat Plate) for Stagnation-Temperature Range 4100 to 8300°R," NASA TN D-54 (1959).

8. Savage, R. T., and C. L. Jaeck, "Investigation of Turbulent Heat Transfer at Hypersonic Speeds," AFFDL-TR-67-144, Vol. 1 (1967).

9. Eckert, E. R. G., "Survey on Heat Transfer at High Speeds," WADC Technical Report 54-70 (1954).

10. Quinn, R. D., and M. Palitz, "Comparison of Measured and Calculated Turbulent Heat Transfer on the X-15 Airplane at Angles of Attack to 19°," NASA TM X-1291 (Confidential).

11. Spalding, D. B., and S. W. Chi, "The Drag of a Compressible Turbulent Boundary Layer on a Smooth Flat Plate With and Without Heat Transfer," J. Fluid Mech. 18 (1), pp. 117-143 (1964).

12. Schlichting, H., Boundary Layer Theory, McGraw-Hill, New York 4th Edition, p. 537 (1960).

13. Dhawan, S., and R. Narasimha, "Some Properties of Boundary Layer Flow During the Transition from Laminar to Turbulent Motion," J. Fluid Mech. 3 (4), p. 418-436.

14. Reynolds, W. E., W. M. Kays, and S. J. Kline, "Heat Transfer in the Turbulent Incompressible Boundary Layer, IV-Effect of Location of Transition and Prediction of Heat Transfer in a Known Transition Region," NASA Memo 12-4-58W (1958).

15. Henderson, Arthur, Jr., "Hypersonic Viscous Flows," Chapter 3 in Modern Developments in Gas Dynamics, Plenum Press, p. 116 (1969).

16. Polek, T. E., and G. G. Mateer, "Measurements of Turbulent Heat Transfer on Cones and Swept Plates at Angle of Attack in Compressible Turbulent Boundary Layers," NASA SP-216, p. 455 (1968).

AEROSPACE CORPORATION

INTERNAL DISTRIBUTION LIST

(REFERENCE: COMPANY PRACTICE 7-21-1)

REPORT TITLE

A COMPARISON OF FOUR SIMPLE CALCULATION METHODS FOR THE COMPRESSIBLE TURBULENT BOUNDARY LAYER ON A FLAT PLATE

REPORT NO.	PUBLICATION DATE	SECURITY CLASSIFICATION
TOR-0066(5758-02)-3	70 MAR 16	Unclassified

(NOTE: FOR OFF-SITE PERSONNEL, SHOW LOCATION SYMBOL, e.g. JOHN Q. PUBLIC/VAFB)

G. N. Freeman
O. Kramer
D. E. Lapedes
M. Masaki
H. Mirels
N. R. O'Brien
E. I. Pritchard
W. F. Radcliffe
I. Rattinger
J. Vasiliu (5)
H. E. Wang
W. R. Warren, Jr.
J. K. Yakura (20)
John Ellinwood
W. King
J. H. Ashmore
R. H. Herndon

APPROVED BY W F Radcliffe DATE

SHEET ____ OF ____

AEROSPACE FORM 2394 REV 7-66

AEROSPACE CORPORATION

EXTERNAL DISTRIBUTION LIST

(REFERENCE: COMPANY PRACTICE 7-21-1)

REPORT TITLE
A COMPARISON OF FOUR SIMPLE CALCULATION METHODS FOR THE COMPRESSIBLE TURBULENT BOUNDARY LAYER ON A FLAT PLATE

REPORT NO.	PUBLICATION DATE	SECURITY CLASSIFICATION
TOR-0066(5758-02)-3	70 MAR 16	Unclassified

MILITARY AND GOVERNMENT OFFICES	ASSOCIATE CONTRACTORS AND OTHERS
(NOTE: SHOW FULL MAILING ADDRESS; INCLUDE ZIP CODE, MILITARY OFFICE SYMBOL, AND "ATTENTION" LINE.)	
Lt. Col. L. Bowles, SMAO (60)	

AFR 310-2 DISTRIBUTION STATEMENTS X'd BELOW APPLY					IF LIST COMPRISES TWO OR MORE SHEETS, COMPLETE THIS SIGNATURE BLOCK ON LAST SHEET ONLY
1. X	2.	3.	4.	5.	

APPROVED BY N.F. Radcliffe F.H. Shelman (FOR AEROSPACE CORPORATION) DATE 3/24/70

APPROVED BY Major O.B. Curtis USAF (FOR COGNIZANT AF OFFICE) SMAOL (SYMBOL) DATE 25 March 70

SHEET ____ OF ____

AEROSPACE FORM 2380 REV 11-66